Available online at www.sciencedirect.com

ScienceDirect

Solar Energy 110 (2014) 781–788

SOLAR ENERGY

www.elsevier.com/locate/solener

Parameter identification of solar cell model using Levenberg–Marquardt algorithm combined with simulated annealing

Fayrouz Dkhichi *, Benyounes Oukarfi, Abderrahim Fakkar, Noureddine Belbounaguia

Electrical Engineering Department, EEA&TI Laboratory, Faculty of Sciences and Techniques, Hassan II Mohammedia-Casablanca University, Mohammedia 28800, Morocco

Received 22 March 2014; received in revised form 22 August 2014; accepted 24 September 2014
Available online 18 November 2014

Communicated by: Associate Editor Elias K. Stefanakos

Abstract

In recent years, several researchers have been interested in looking for accurate parameter identification techniques able to deal with the high non-linearity of the solar cell model. In this regard, we proposed in this paper, the optimization method of Levenberg–Marquardt (LM) combined with simulated annealing (SA). The aspect of combination between the two methods is based on the optimal setting of the damping factor of LM at each iteration by SA. The performance of the proposed approach is tested by identifying the model parameters of a 57 mm diameter commercial (R.T.C. France) silicon solar cell. As a result, the developed approach shows its high accuracy when comparing the obtained outcomes with those reported by the other methods in the literature. This effectiveness is proved by the minimal values of statistical errors and the good agreement between the experimental data and the fitted curve. On the other hand, in an attempt to understand the synergy between LM and SA, we firstly studied in detail the behavior of each one and then the impact of their combination on the parameters evolution during the convergence procedure.

Keywords: Identification; Levenberg–Marquardt; Simulated annealing; Optimization; Solar cell; Electrical parameters

1. Introduction

The general performances of a photovoltaic (PV) generator are prone to be degraded over time, due to exhibition to weather conditions and aging. Therefore, it is important to predict these degradations in order to avoid its harmful influences on the PV power production. In this context, the evaluation of the solar cell behavior under the operating conditions is required.

The solar cell behavior under illumination is interpreted by several models; whose the equivalent electrical circuit based on single diode is the most widely used (Kumar and Panchal, 2013; Fathabadi, 2013; Siddiqui et al., 2013; Rajasekar et al., 2013). This model reflects the implicit non-linear relationship between PV current (I_{PV}), PV voltage (V_{PV}) and the five intrinsic electrical parameters namely series resistance, shunt resistance, photocurrent, saturation current and diode ideality factor. For this purpose, a better modeling of the solar cell requires an appropriate identification technique that provides quite accurate intrinsic parameters.

Among the overall of identification techniques reported in the literature, the numerical methods are more revealing of the real electrical parameters values, since they use all measured points of I_{PV} and V_{PV} forming the $I_{PV}(V_{PV})$ characteristic. This type of methods is based on the

* Corresponding author. Tel.: +212 06 53200413.
E-mail addresses: dkhichi.fayrouz@gmail.com, dkhichi_fayrouz@hotmail.fr (F. Dkhichi), benyounes.oukarfi@univh2m.ac.ma (B. Oukarfi).

http://dx.doi.org/10.1016/j.solener.2014.09.033
0038-092X/

optimization of error between the theoretical and experimental characteristic during the fitting process.

In this paper, we proposed for the parameter identification of the solar cell single diode model, a numerical optimization approach presented by the combination of two different methods: the first one is deterministic based on the gradient descent "Levenberg–Marquardt – LM", whereas the second one is heuristic "Simulated Annealing – SA". In order to ensure an optimal convergence, SA operates as a seeking method of the optimal value of damping factor at each iteration of LM method.

The outcomes obtained by the approach of LM combined with SA (LMSA) are compared with those found by various algorithms used in literature: Global Grouping-based Harmony Search (GGHS) (Askarzadeh and Rezazadeh, 2012), Artificial Bee Swarm Optimization (ABSO) (Askarzadeh and Rezazadeh, 2013), Chaotic Particle Swarm Optimization (CPSO) (Wei et al., 2011), Differential Evolution (DE) (Hachana et al., 2013), Pattern Search (PS) (Al Rashidi et al., 2012a), SA (Al Rashidi et al., 2012b), Genetic Algorithm (GA) (Zagrouba et al., 2010) and Newton–Raphson (Easwarakhanthan et al., 1986). The high accuracy of LMSA shows its ability and its efficiency to identify the most accurate values of the model parameters of commercial solar cell (R.T.C. France), based on $(I_{PV} - V_{PV})$ experimental data.

However, to know how the LMSA algorithm reaches such accuracy in the parameter identification, we therefore shed light on its convergence procedure. We studied, by providing further details, the behavior of LMSA and the influence of SA algorithm at the different steps of LM algorithm during the parameter identification process.

The rest of the paper is mainly organized as follows: Section 2 describes the solar cell modeling. In Section 3 we firstly introduce the minimized objective function then we explain why we especially used SA in the combination with LM. Thereafter, in the same section, we define the LMSA algorithm used in this study. The Section 4 presents the obtained results and the related discussions, while the Section 5 gives a conclusion of the paper.

2. Single diode equivalent model of solar cell under illumination

The single diode equivalent circuit model of solar cell used in this study is presented in Fig. 1. For a given temperature and illumination, the current source converts the absorbed light photons to a photocurrent I_{ph}. The latter brings up a leakage current at the PN junction. Furthermore, the defects presented by the materials of this junction and the losses which are due to different contacts and connections are respectively modeled by the shunt resistance R_{sh} and series resistance R_s. The diode used is characterized by two intrinsic parameters which are the saturation current I_s and the ideality factor n. The characteristic

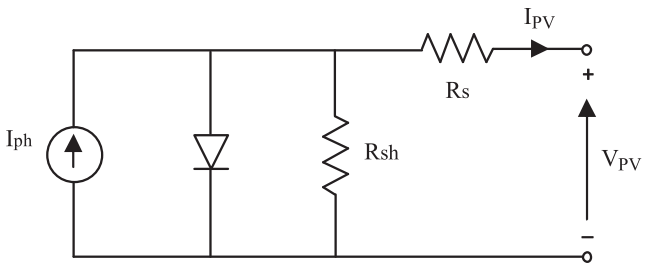

Fig. 1. The single diode equivalent electrical model of solar cell.

$I_{PV}(V_{PV})$ generated by the solar cell is obtained by placing a variable load at the output of the cell.

The mathematical model, basically derived from the above circuit, allows the calculation of the I_{PV} according to the five intrinsic electrical parameters values, by the following expression:

$$I_{PV} = I_{ph} - I_s\left[\exp\left(\frac{V_{PV} + R_s I_{PV}}{nV_{th}}\right) - 1\right] - \frac{V_{PV} + R_s I_{PV}}{R_{sh}} = f(I_{PV}, V_{PV}, \theta) \quad (1)$$

where

V_{th}: Thermal voltage (A.T)/q,
A: Boltzmann constant ($1.3806503 \times 10^{-23}$ J/K),
q: Charge of the electron ($1.6021764 \times 10^{-19}$ C),
T: Temperature of the cell in Kelvin.

3. Parameter identification process

3.1. Optimization principle

In order to identify the intrinsic parameters R_s, R_{sh}, I_{ph}, I_s and n from the $I_{PV}(V_{PV})$ characteristic, we fitted to the best the model of Eq. (1) to the experimental data $(I_{PV} - V_{PV})$, through the minimization of squared errors between the theoretical and experimental curves. Therefore, the objective function used in the optimization process is the Sum of Squared Error (SSE), which is given as:

$$g(I_{PV}, V_{PV}, \theta) = \sum_{i=1}^{N}\left[I_{PVmes\ i} - f(I_{PV}, V_{PV}, \theta)_i\right]^2 = \sum_{i=1}^{N}\left[\varepsilon(I_{PV}, V_{PV}, \theta)_i\right]^2 \quad (2)$$

where

$I_{PVmes\ i}$: Present the ith measured value of I_{PV},
ε: Error between $I_{PVmes\ i}$ and I_{PV} calculated by $f(I_{PV}, V_{PV}, \theta)$ from Eq. (1),
N: Number of the measurement points,
θ: Vector of the five intrinsic parameters R_s, R_{sh}, I_{ph}, I_s and n.

The minimum of SSE leads to five optimal values of the parameters θ.

The minimization of the objective function cannot be done in analytically intuitive way due to the strong non-linearity of the characteristic $I_{PV}(V_{PV})$. Indeed, we noteworthy that the solar cell model has a double non-linearity. The first one is inherent to the Eq. (1) itself, while the second one is of the structural parameters R_s and n. Hence, the numerical methods for the nonlinear regression based on the least squares principle are more appropriate to minimize such function.

3.2. Levenberg–Marquardt method combined with simulated annealing

3.2.1. Levenberg–Marquardt method

The traditional method of LM has the advantage to behave as two methods based on different orders of gradient: "steepest descent" and "Gauss–Newton" (Lourakis, 2005; Lampton, 1997; Lourakis and Argyros, 2005) having complementary features. Effectively, the LM method begins with the steepest descent to take benefit of its low sensitivity toward initial values. Then, once the calculated values become in close proximity of the final solution, it is Gauss–Newton that takes over, allowing a fast convergence rate. Automatic switching of the steepest descent to Gauss–Newton within the LM method is ensured by the control parameter λ named "damping factor". Therefore, the parameters θ to be identified, are updated at each iteration according to the hereafter expression:

$$\theta_{k+1} = \theta_k - \left[\frac{J'\varepsilon}{J'J + \lambda_k I}\right]_{\theta=\theta_k} \quad (3)$$

where

J: Jacobian matrix $\left(\frac{\partial f(\theta)}{\partial \theta}\right)_{\theta=\theta_k}$, contains the derivatives of the function $f(I_{PV}, V_{PV}, \theta)$ according to each parameter of the vector θ,
I: Identity matrix.

3.2.2. Evolution of the damping factor λ

The damping factor $\lambda > 0$ whose the value must be determined at each iteration of LM, plays a crucial role in leading the convergence procedure of the algorithm. Indeed, when LM is in steepest descent stage, the factor λ takes an important values and the Hessian matrix $(J'J + \lambda_k I)$ in Eq. (3) becomes dominant in diagonal. However, when LM is in Gauss–Newton stage, λ changes automatically and takes rather small values, this entails that the Hessian $J'J$ outweighs the matrix $\lambda_k I$.

In literature, the setting of the damping factor λ is usually done by the method based on updating this factor by λ/v or by $\lambda \cdot v$, depending on whether the objective function decreases or increases. v denotes a constant value, determined by trial, the most assigned value to this constant is 10 (Bledsoe et al., 2011; Francioli et al., 2010). By using the above classical method to control λ values, the LM algorithm does not always converge to the optimal parameters θ and this was tested when we have given several times to this algorithm different initial values of the five parameters, no matter if they are close to the solution θ. In this case, the inability of LM can be explained by the use of non-optimal values of λ found by the classical method. Hence, in the aim to remedy this drawback, we undertook a detailed investigation of the factor λ.

Effectively, we studied the evolution of the function $g(I_{PV}, V_{PV}, \theta_k, \lambda)$ (denoted by $g(\lambda)$ for θ fixed at θ_k) according to different values of λ, at each iteration k of LM algorithm. Therefore we observed, at each step k, the presence of several local minimums of $g(\lambda)$. For this purpose and in order to determine the global minimum of $g(\lambda)$ corresponding to the best minimization of the objective function $g(I_{PV}, V_{PV}, \theta)$ (denoted by $g(\theta)$), at each iteration k, we thought to use the SA method.

3.2.3. Principle of simulated annealing method

SA is a heuristic optimization method that allows getting out from the pitfalls of local minimums for falling into the global minimum (Fig. 2).

At one iteration k of LM, the SA method introduces random perturbations on the value of the damping factor λ and evaluates the corresponding value of the $g(\lambda)$. Still at the same iteration k, the decreased values of this function with regard to its initial value are accepted and those increased, which represent the bad values, are rejected. This evaluation process is carried out based on the "Mitropolis condition". According to this criterion, some values of λ whose $g(\lambda)$ is increased are tolerated. The acceptance of the bad values of λ allows to SA to not get stuck in the local minimums and move towards the global minimum. When this one is reached, the SA method gives then the corresponding damping factor λ which is the optimal value at the current iteration k, such as:

$$g(\lambda_{opt}) = min_{global}\left[g(\lambda)_{\theta=\theta_k}\right] \quad (4)$$

The process of SA described above is then performed at each iteration of LM. Therefore, the determined value of λ_{opt} used in Eq. (3) at an iteration k, allows to lead the objective function $g(\theta)$ to a best minimization at an

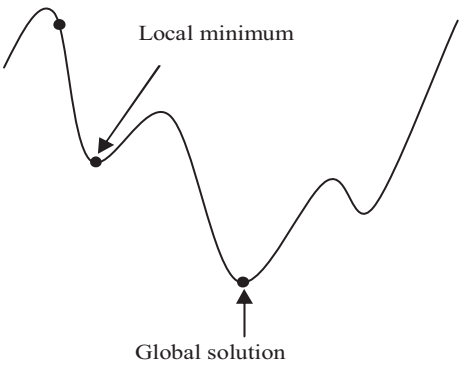

Fig. 2. Simulated annealing principle.

iteration $k+1$ due to the precise value of $\lambda_k = \lambda_{opt}$ determined by SA. The algorithm of SA that we used into LMSA is that presented by Al Rashidi et al. (2012b).

3.2.4. Initialization method

The initialization of unknown parameters is important for the convergence of an optimization algorithm, as is the case with GGHS, ABSO, CPSO, DE, Newton, PS, SA and GA algorithms (Askarzadeh and Rezazadeh, 2012, 2013; Wei et al., 2011; Hachana et al., 2013; Easwarakhanthan et al., 1986; Al Rashidi et al., 2012a,b; Zagrouba et al., 2010). In this regard, we have chosen in this paper the linear least squares method (LSM) to initialize the five parameters for LMSA algorithm. The advantage of this method is that it is direct and not iterative. However, it is normally applicable only to linear systems with respect to parameters. This property is not verified for our characteristic $I_{PV}(V_{PV})$. However, we note that it has two regions: Linear and non-linear. For the first region, the LSM method is applied merely, while in the non-linear region, we can by a suitable approximation make a linearization in a logarithmic way (Bouzidi et al., 2007).

3.2.5. LMSA algorithm

The LMSA algorithm is presented step by step in Fig. 3. Where g (θ) is the objective function $g(I_{PV}, V_{PV}, \theta)$ that varies according to θ.

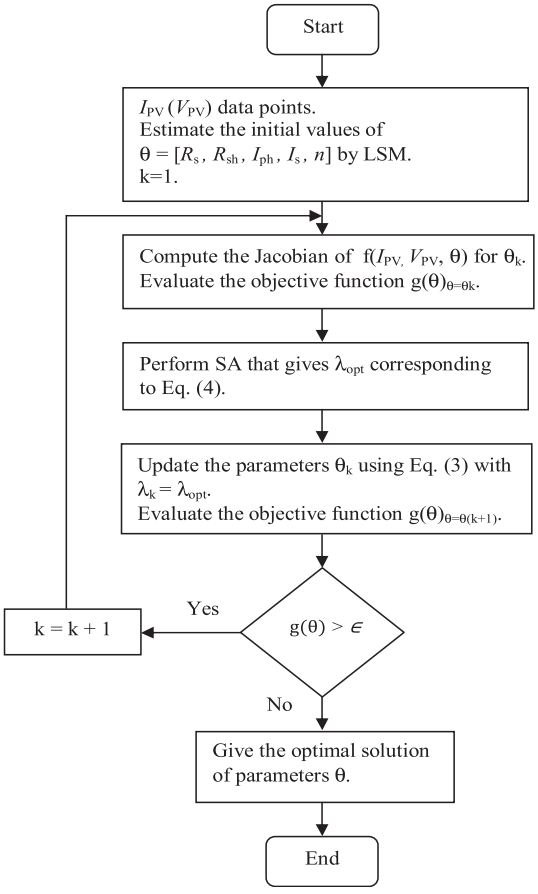

Fig. 3. Flowchart of the LMSA algorithm for parameter identification of single diode solar cell model.

The convergence procedure of LMSA is stopped when a precision ϵ is reached.

4. Results and discussions

In order to study the performance of LMSA method in parameter identification, we consider the single diode solar cell model. The experimental measurements $(I_{PV} - V_{PV})$ used are reported by Easwarakhanthan et al. (1986), which correspond the 57 mm diameter commercial (R.T.C. France) silicon solar cell and they are taken at a temperature of 33 °C and an illumination of 1000 W/m^2.

The identification process carried out by LMSA algorithm is implemented and executed in Matlab environment.

4.1. Trend of λ factor

As a first step, we conducted a linear search of the damping factor λ at each iteration of LM, by sweeping all values of this factor to know its impact on the function $g(\lambda)$.

Fig. 4 clearly shows that the evolution of the function $g(\lambda)$ at an iteration k includes four minimums in which one is global. The existence of multiple minimums is also observed in the evolution of each $g(\lambda)$ at each iteration of LM algorithm. It is on this basis that the SA method has been proposed to determine the correct value of λ.

4.2. Statistical criteria

In order to assess the fit of the model with experimental data, two basic statistical functions are used. They provide a detailed analysis about accuracy of the results of the parameter identification. The statistical criteria used are:

- Root Mean Squared Error (RMSE):

$$RMSE = \sqrt{\frac{1}{N}\sum_{i=1}^{N}\left[I_{PVmes\ i} - f(I_{PV}, V_{PV}, \theta)_i\right]^2}$$

- Individual Absolute Error (IAE):

$$IAE_i = \left|I_{PVmes\ i} - f(I_{PV}, V_{PV}, \theta)_i\right|$$

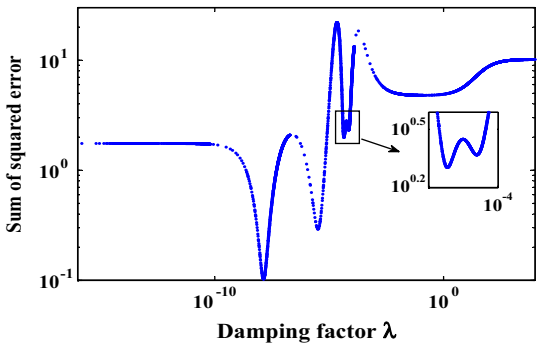

Fig. 4. The evolution of the function $g(\lambda)$.

Table 1
Results obtained by LMSA and those of other methods for single diode model of commercial solar cell.

Item	GA	SA	PS	Newton	DE	CPSO	ABSO	GGHS	LMSA
R_s (Ω)	0.0299	0.0345	0.0313	0.0364	0.0364	0.0354	0.0366	0.0363	0.03643
R_{sh} (Ω)	42.3729	43.1034	64.1026	53.7634	53.7185	59.012	52.2903	53.0647	53.32644
I_{ph} (A)	0.7619	0.7620	0.7617	0.7608	0.7608	0.7607	0.7608	0.7609	0.76078
I_s (μA)	0.8087	0.4798	0.9980	0.3223	0.3230	0.4000	0.3062	0.3262	0.31849
n	1.5751	1.5172	1.6000	1.4837	1.4806	1.5033	1.4758	1.4822	1.47976
Statistical criteria									
SSE	9.4632e−3	9.3839e−3	5.8005e−3	2.4445e−3	1.4265e−4	4.9952e−5	2.5547e−5	2.5528e−5	***2.5297e−5***
RMSE	1.9078e−2	1.8998e−2	1.4936e−2	9.6964e−3	2.3423e−3	1.3861e−3	9.9124e−4	9.9097e−4	***9.8640e−4***

4.3. Accuracy of results

The identification results obtained by the proposed LMSA are compared with those of GGHS (Askarzadeh and Rezazadeh, 2012), ABSO (Askarzadeh and Rezazadeh, 2013), CPSO (Wei et al., 2011), DE (Hachana et al., 2013), Newton (Easwarakhanthan et al., 1986), PS (Al Rashidi et al., 2012a), SA (Al Rashidi et al., 2012b) and GA (Zagrouba et al., 2010). These methods were chosen for comparing, because they present the latest and the most accurate results in the field of parameters identification of the solar cell.

It is clearly seen from the results in Table 1 that the five electrical parameters identified by the LMSA method are quite close and more accurate than those found by the other reported methods. The high accuracy of the identified parameters is denoted by the best value of RMSE which is highlighted by bold italic size. As a result, LMSA outperforms the overall of the compared methods, which are ranked in order by GGHS, ABSO, CPSO, DE, Newton, PS, SA and GA.

The minimal value of the objective function indicates that the parameters identified are quite close to the real ones. Then to evaluate the value of this criterion for each compared method, the corresponding set of the five parameters is substituted in Eq. (1). After performing the calculation, it appears that the LMSA yields the best value of SSE among the calculated values for the other methods.

We consider in Table 2 the three most accurate algorithms (GGHS, ABSO and CPSO). As it is seen, the LMSA provides the minimal value of the sum of IAE compared to those algorithms.

Table 2
Fitting results of I_{PV} calculated and of IAE obtained by LMSA, GGHS, ABSO and CPSO for single diode model of commercial solar cell.

Measurement	V_{PV} (V)	I_{PV} measured (A)	I_{PV} calculated (A)	IAE based on LMSA	IAE based on GGHS	IAE based on ABSO	IAE based on CPSO
1	−0.2057	0.7640	0.76411576150	0.00011576150	0.00025409278	0.00019935790	0.00027217949
2	−0.1291	0.7620	0.76268067173	0.00068067173	0.00081191916	0.00073583937	0.00043095315
3	−0.0588	0.7605	0.76136328121	0.00086328122	0.00098802489	0.00089235619	0.00074042125
4	0.0057	0.7605	0.76084685590	0.00034685592	0.00022809004	0.00034172848	0.00035330824
5	0.0646	0.7600	0.76095366919	0.00095366920	0.00084039554	0.00097034535	0.00085421841
6	0.1185	0.7590	0.75997381266	0.00097381267	0.00086567039	0.00101025408	0.00077860172
7	0.1678	0.7570	0.75706902713	0.00006902714	0.00017218849	0.00001501708	0.00034872884
8	0.2132	0.7570	0.75788677760	0.00088677761	0.00078890515	0.00095578587	0.00053641061
9	0.2545	0.7555	0.75594530712	0.00044530712	0.00035371275	0.00052534586	0.00004611844
10	0.2924	0.7540	0.75421933880	0.00037013881	0.00028703709	0.00045535705	0.00004506813
11	0.3269	0.7505	0.75120832909	0.00085842909	0.00092942384	0.00077674784	0.00124114833
12	0.3585	0.7465	0.74717804496	0.00082734496	0.00088124037	0.00076091219	0.00111360859
13	0.3873	0.7385	0.73995443010	0.00160213011	0.00163391043	0.00156430520	0.00172219053
14	0.4137	0.7280	0.72847073736	0.00061633736	0.00060919035	0.00061399772	0.00071586669
15	0.4373	0.7065	0.70685162273	0.00049292273	0.00047948093	0.00053844672	0.00017570550
16	0.4590	0.6755	0.67554738591	0.00018248591	0.00020348191	0.00010313989	0.00063623776
17	0.4784	0.6320	0.63306850572	0.00119490573	0.00120107364	0.00110693294	0.00161039255
18	0.4960	0.5730	0.57391195223	0.00102655224	0.00099218825	0.00096348220	0.00118099851
19	0.5119	0.4990	0.49953910213	0.00063890213	0.00073414479	0.00016460262	0.00094821681
20	0.5265	0.4130	0.41357497991	0.00065757991	0.00082600199	0.00243286509	0.00158721310
21	0.5398	0.3165	0.31742907916	0.00099237917	0.00122715161	0.00018453268	0.00255846843
22	0.5521	0.2120	0.21207038272	0.00011278272	0.00039237935	0.00015697066	0.00222110541
23	0.5633	0.1035	0.10478529286	0.00130599286	0.00102001176	0.00154635825	0.00111046983
24	0.5736	−0.0100	−0.0112265833	0.00122858334	0.00146201323	0.00103236042	0.00354617357
25	0.5833	−0.1230	−0.1255206475	0.00254524758	0.00240976375	0.00272459412	0.00061781930
26	0.5900	−0.2100	−0.2114805121	0.00152251211	0.00152951102	0.00155921247	0.00273840144
Sum of IAE				0.02151039086	0.02212100352	0.022330848332	0.02813002468

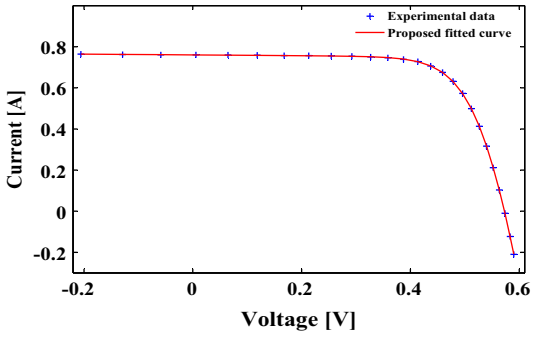

Fig. 5. Experimental data of $I_{PV}(V_{PV})$ and proposed fitted curve for the commercial solar cell.

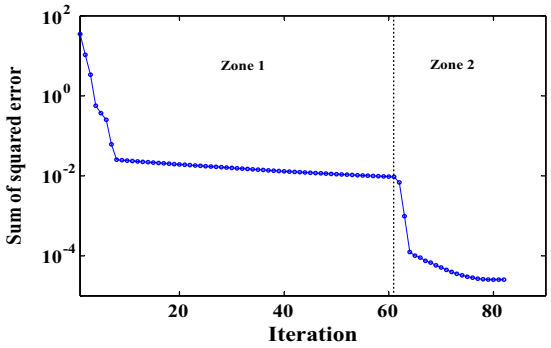

Fig. 6. Trend of the objective function obtained by LMSA algorithm.

Always, in order to confirm the effectiveness of LMSA in providing better accuracy, we plotted the experimental and calculated values of $I_{PV}(V_{PV})$ in Fig. 5. From this figure we can clearly see that the two curves fit very well.

4.4. Process of convergence

4.4.1. Trend of the objective function by LMSA algorithm

The evolution of the objective function SSE fully reflects the behavior of the LMSA algorithm during the convergence process. It seems evident from Fig. 6 that the evolution of SSE, obtained after running LMSA algorithm, brings together two distinct key zones:

- Zone 1: LMSA behaves during the first iterations as steepest descent algorithm, which explains the slow convergence. Effectively, this algorithm, which is known by its low sensitivity toward initial values, refine slowly (between the 8th and the 61st iteration) the five parameters and bring them near to optimal values with a SSE value around $1e^{-2}$.
- Zone 2: the objective function shows a sharp decrease at the 61st iteration. The convergence rate of LMSA becomes fast by behaving as Gauss–Newton algorithm, known for its fast convergence when the values that they are supplied are around the optimum.

Automatic failover of steepest descent to Gauss–Newton into LMSA is performed using the values of damping factor λ determined by the SA method. The optimal values of λ found in the iterations of the LMSA algorithm are shown in Fig. 7.

The sharp minimization of the objective function SSE in the first iterations of the graph in Fig. 6, is explained by large values of λ. Followed then by a slow convergence between the 8th and the 61st iteration due to values around to 1 of this factor. The sharp bearish of the SSE at the beginning of zone 2 is resulted by the production of small values of λ less than 1 (between $1e^{-6}$ and $1e^{-18}$).

It is clearly seen that LMSA algorithm required 82 iterations to converge to the optimal values of electrical

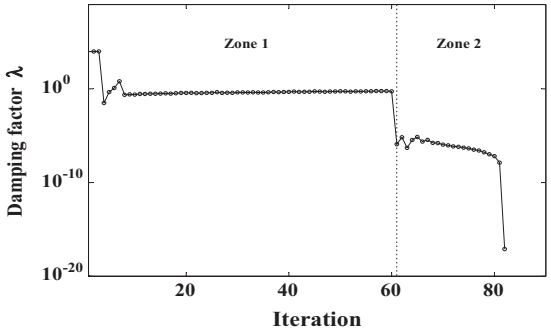

Fig. 7. Trend of damping factor λ obtained by LMSA algorithm.

parameters. Nevertheless, if we take into account the number of iterations of SA at each step of LM, therefore, the LMSA does 2050 iterations to converge from the initial values of the five parameters (with SSE = 35.9348 and RMSE = 1.1767), towards the optimal values of the five parameters (with SSE = $2.5297e^{-5}$ and RMSE = $9.8640e^{-4}$).

Since the SA considered in this study is a one-dimensional optimization method, therefore, it was performed to determine factor λ value in order to provide a proper minimization of the objective function, at each iteration of LM.

4.4.2. Behavior of LMSA on the electrical parameters

Figs. 8–12 show that the evolutions of the five parameters R_s, R_{sh}, I_{ph}, I_s, and n are marked by a transitional stage between the 4th and the 8th iteration that allows to the objective function in Fig. 6 to continue its rough minimization until the 8th iteration. Just after, this minimizing becomes slow.

The slow convergence is also observed in the evolutions of the five parameters between the 8th and the 61st iteration. Such as the values of parameters R_s, I_s and n, defining the non-linear part of Eq. (1), are changed gradually (Figs. 8, 11 and 12), while the values of the two linear parameters R_{sh} and I_{ph}, are changed slightly (Figs. 9 and 10). These different trends could be explained by the effect of non-linear steepest descent algorithm (characterizing

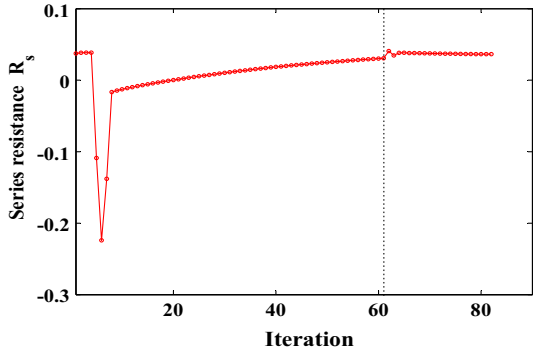

Fig. 8. Trend of series resistance R_s (Ω).

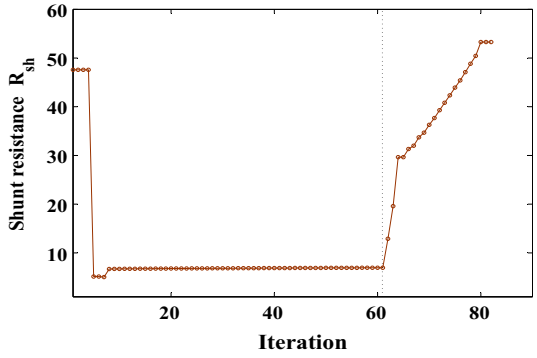

Fig. 9. Trend of shunt resistance R_{sh} (Ω).

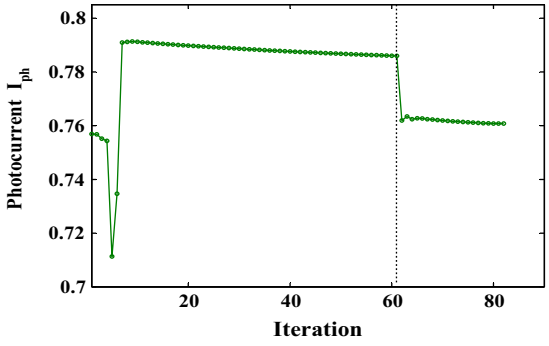

Fig. 10. Trend of photocurrent I_{ph} (A).

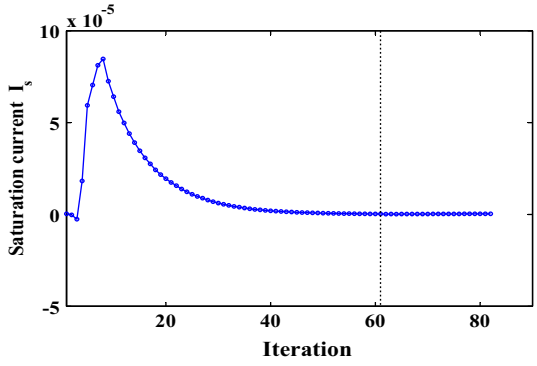

Fig. 11. Trend of saturation current I_s (A).

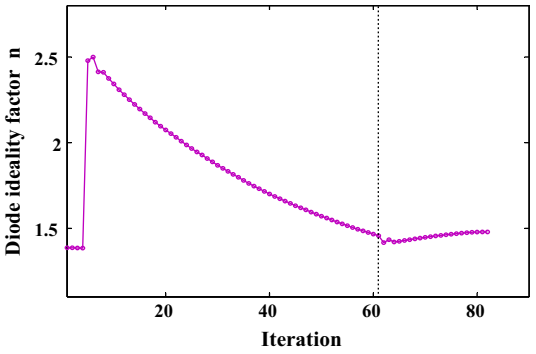

Fig. 12. Trend of diode ideality factor n.

LMSA in the first zone) to change the nonlinear parameters without the linear ones. As a result, the steepest descent refine, to the best, the values of the three parameters R_s, I_s and n and bring them near to the optimum. This behavior of steepest descent towards the non-linear parameters, could explain the ability of this algorithm to be less sensitive to the initial values. On the other hand, as it is clearly shown in Figs. 9 and 10, between the 8th and the 61st iteration, R_{sh} and I_{ph} parameters have evolved in two opposite directions relative to each other. This behavior could be explained by a compensation between the linear parameters R_{sh} and I_{ph}, which could provide the suitable values of these two parameters that allow to LMSA to change the non-linear parameters R_s, I_s and n, during the same phase of number of iterations.

Although, LMSA began from the 62nd iteration to vary the parameters R_{sh} and I_{ph} when the parameters R_s, I_s and n become properly adjusted close to the optimal values as it is seen in Figs. 8–12. Therefore, LMSA converges quickly until the end of the convergence, which proves that the Gauss–Newton algorithm (characterizing LMSA in the second zone) is especially sensitive to the initial values of the non-linear parameters more than the linear ones.

5. Conclusion

The main aim of this paper is to develop an efficient LM algorithm able to identify the accurate parameters of the solar cell model. To do so, we used the SA method to determine automatically at each iteration of LM, the optimal value of the damping factor, ensuring a good minimization of the objective. The SA is more reliable and robust in term of providing right value of λ in order to converge towards the optimal values of the five parameters, unlike the classical method which is usually used into LM to estimate λ and which showed his inability to lead the convergence of LM. The combination between LM and SA named by LMSA algorithm, lead to accurate parameters of the single diode model. This high accuracy was revealed after the comparison of the obtained results with those of the other methods reported previously. Moreover, it was confirmed when the fitted values of $I_{PV}(V_{PV})$ match very well with experimental data. In order to shed the light in the synergy

between LM and SA and give detailed information about the behavior of LMSA algorithm, a further investigation is made, by showing and explaining the trends of the objective function and of the five parameters.

The LMSA is a potential algorithm that can be efficiently applied for the parameter identification of the double diode solar cell model and also of the module model.

Moreover, to minimize the dependence of LMSA to the initial values, we propose a modified LMSA algorithm which should be more robust, faster and less sensitive to initial values. In this regard, first encouraging results have been shown. A more rigorous study is underway to confirm this hypothesis

References

Al Rashidi, M., Al Hajri, M., El-Naggar, K., Al-Othman, A., 2012a. Optimal extraction of solar cell parameters using pattern search. Renew. Energy 44, 238–245.

Al Rashidi, M., El-Naggar, K., Al Hajri, M., Al-Othman, A., 2012b. Simulated annealing algorithm for photovoltaic parameters identification. Sol. Energy 86 (1), 266–274.

Askarzadeh, A., Rezazadeh, A., 2012. Parameter identification for solar cell models using harmony search-based algorithms. Sol. Energy 86 (11), 3241–3249.

Askarzadeh, A., Rezazadeh, A., 2013. Artificial bee swarm optimization algorithm for parameters identification of solar cell models. Appl. Energy 102, 943–949.

Bledsoe, K.C., Favorite, J.A., Aldemir, T., 2011. A comparison of the covariance matrix adaptation evolution strategy and the Levenberg–Marquardt method for solving multidimensional inverse transport problems. Ann. Nucl. Energy 38 (4), 897–904.

Bouzidi, K., Chegaar, M., Bouhemadou, A., 2007. Solar cells parameters evaluation considering the series and shunt resistance. Sol. Energy Mater. Sol. Cells 91 (18), 1647–1651.

Easwarakhanthan, T., Bottin, J., Bouhouch, I., Boutrit, C., 1986. Nonlinear minimization algorithm for determining the solar cell parameters with microcomputers. Int. J. Sol. Energy 4 (1), 1–12.

Fathabadi, H., 2013. Novel neural-analytical method for determining silicon/plastic solar cells and modules characteristics. Energy Convers. Manage. 76, 253–259.

Francioli, L., Knobel, R., Kurnik, R.T., 2010. PCR Elbow Determination by use of a Double Sigmoid Function Curve Fit with the Levenburg–Marquardt Algorithm and Normalization. US Patent 7,680,868.

Hachana, O., Hemsas, K., Tina, G., Ventura, C., 2013. Comparison of different metaheuristic algorithms for parameter identification of photovoltaic cell/module. J. Renew. Sust. Energy 5 (5), 053122.

Kumar, G., Panchal, A.K., 2013. A non-iterative technique for determination of solar cell parameters from the light generated IV characteristic. J. Appl. Phys. 114 (8), 084904.

Lampton, M., 1997. Damping–undamping strategies for the Levenberg–Marquardt nonlinear least-squares method. Comput. Phys. 11 (1), 110–115.

Lourakis, M.I., 2005. A brief description of the Levenberg–Marquardt algorithm implemented by levmar. Found. Res. Technol. 4, 1–6.

Lourakis, M.I., Argyros, A.A., 2005. Is Levenberg–Marquardt the most efficient optimization algorithm for implementing bundle adjustment? In: Tenth IEEE International Conference on Computer Vision, 2005. ICCV 2005, vol. 2. IEEE, pp. 1526–1531.

Rajasekar, N., Krishna Kumar, N., Venugopalan, R., 2013. Bacterial foraging algorithm based solar PV parameter estimation. Sol. Energy 97, 255–265.

Siddiqui, M., Arif, A., Bilton, A., Dubowsky, S., Elshafei, M., 2013. An improved electric circuit model for photovoltaic modules based on sensitivity analysis. Sol. Energy 90, 29–42.

Wei, H., Cong, J., Lingyun, X., Deyun, S., 2011. Extracting solar cell model parameters based on chaos particle swarm algorithm. In: 2011 International Conference on Electric Information and Control Engineering (ICEICE). IEEE, pp. 398–402.

Zagrouba, M., Sellami, A., Bouaïcha, M., Ksouri, M., 2010. Identification of PV solar cells and modules parameters using the genetic algorithms: application to maximum power extraction. Sol. Energy 84 (5), 860–866.